

# Orbitally relieved magnetic frustration in $\text{NaVO}_2$

Ting Jia, Guoren Zhang and Zhi Zeng\*

*Key Laboratory of Materials Physics, Institute of Solid State Physics,  
Chinese Academy of Sciences, Hefei 230031, P. R. China*

H. Q. Lin

*Department of Physics and Institute of Theoretical Physics,  
The Chinese University of Hong Kong, Shatin, Hong Kong, P. R. China*

(Dated: February 3, 2022)

The magnetic properties of  $\text{NaVO}_2$  are investigated using full-potential linearized augmented plane wave method. We perform calculations for three structures. For the rhombohedral structure at 100 K, the  $t_{2g}$  orbitals of V ions are split into upper  $a_{1g}$  and lower  $e'_g$  orbitals by a trigonal distortion of compression. For the monoclinic structure at 91.5 K, the system behaves like a frustrated spin lattice with spatially anisotropic exchange interactions. For another monoclinic structure at 20 K, the magnetic frustration is relieved by a lattice distortion which is driven by a certain orbital ordering, and the long-range magnetic ordering is thus formed. Moreover, the small magnetic moment originates from the compensation of orbital moment for the spin moment.

---

\* Correspondence author: zzeng@theory.issp.ac.cn

## I. INTRODUCTION

The compounds with a common chemical formula  $ATO_2$  ( $A=\text{Na}$  or  $\text{Li}$ ,  $T=3d$  transition metals) have been attracting a lot of attention for their large variety and richness in physical phenomena[1, 2, 3, 4, 5, 6]. Indeed, the discovery of superconductivity in the  $\text{Na}_{0.35}\text{CoO}_2 \cdot 1.3\text{H}_2\text{O}$ [1] and the application of  $\text{LiCoO}_2$  in rechargeable Li batteries have accelerated investigations on their fundamental physics. In addition,  $\text{NaMnO}_2$  undergoes a structural phase transition at 45 K to a long-range ordered antiferromagnetic (AFM) ground state[2], while  $\text{NaNiO}_2$  exhibits ferromagnetic (FM) coupling in Ni-Ni plane below transition temperature[3]. Furthermore, a well-known member of this group,  $\text{LiNiO}_2$ , has no long-range magnetic ordering even at low temperatures[4, 7, 8, 9]. The orbital frustration has been used to explain the absence of magnetic ordering[4, 7, 8], and a local ordering of  $\text{Ni}^{3+}$  Jahn-Teller (J-T) orbitals is also proposed to be responsible for the complex magnetic properties[9]. Therefore, its controversial magnetic properties have been attracting considerable interest.

These various phenomena always relate to the quasi-two-dimensional (2D) triangular lattice formed by  $T$  cations. Such a triangular lattice may lead to magnetic frustration, since all nearest-neighbor AFM interactions can not be satisfied simultaneously[2, 5, 6]. Nevertheless, the magnetic frustration can be relieved by a certain orbital ordering (OO)[10, 11, 12], such as in  $\text{LiVO}_2$ [13] and  $\text{NaVO}_2$ [14].  $\text{LiVO}_2$  has been found to form a spin-singlet phase with corresponding OO at low temperatures[5, 13]. Whereas, its sister compound  $\text{NaVO}_2$  displays very different behaviours.

Recently, Onoda *et al.*[15] have revealed a superparamagnetic state driven by the short-range ordered spin-1 (the total spin in one trimer  $S=1$ ) trimerization[16] below the transition temperature ( $T=98$  K). However, McQueen *et al.* have reported two successive OO transitions in  $\text{NaVO}_2$ [14]. At 98 K, the system undergoes a continuous phase transition from a rhombohedral ( $R\bar{3}m$ ) phase to a monoclinic ( $C2/m$ ) one, corresponding to the proposed OO of one electron per  $\text{V}^{3+}$ . Below 93 K, the system undergoes a discontinuous phase transition to another monoclinic ( $C2/m$ ) phase, consistent with the proposed OO of two electron per  $\text{V}^{3+}$ . In addition, a long-range ordered AFM state is formed at low temperatures, while the magnetic moment observed in the ordered phase is about  $0.98 \mu_B$ , much smaller than the expected value ( $2 \mu_B$ ). The controversial magnetic states below 98 K obtained by these two groups bring us interests, and the puzzling magnetic moment deserves to be explored. There are no theoretical reports yet to the best of our knowledge, therefore we expect to understand its magnetic properties at low temperatures upon our theoretical efforts.

In the present work, we have performed first-principles calculations to investigate the electronic structures of  $\text{NaVO}_2$ , further to reveal the most possible orbital and magnetic ordering, and to explore the origin of small magnetic moment observed at low temperatures. Partially in agreement with the experimental findings[14], the OO, accompanied by a long-range magnetic ordering, is found for the second monoclinic structure. And the observed magnetic moment can be explained by including the spin-orbit coupling (SOC) interactions.

This paper is organized as follows. The crystal structure and computational details are described briefly in Sec. II. And the results and discussions are presented in Sec. III. Finally, a brief conclusion is summarized in Sec. IV.

## II. CRYSTAL STRUCTURE AND COMPUTATIONAL DETAILS

The lattice parameters provided by McQueen *et al.* are listed in Table I. The structure of  $\text{NaVO}_2$  is composed of 2D triangular-lattice  $\text{VO}_2$  layers of edge sharing  $\text{VO}_6$  octahedra separated by sodium ions, which is rhombohedral ( $R-3m$ ) at relatively high temperature (HT) ( $T > 98$  K) and monoclinic ( $C2/m$ ) in both intermediate temperature (IT) ( $91.5 \text{ K} < T < 98 \text{ K}$ ) and low temperature (LT) ( $T < 91.5 \text{ K}$ ) phases[14]. At 100 K, the V-O distances are nearly  $2.04 \text{ \AA}$ , but the O-V-O angle  $\alpha$  is only  $85.53^\circ$  (Fig. 1). With lowering the temperature,  $\alpha$  further reduces to  $85.42^\circ$  at 91.5 K and  $85.13^\circ$  at 20 K. Therefore, even in the HT phase,  $\text{VO}_6$  octahedra in  $\text{NaVO}_2$  have been different from the regular ones under a trigonal distortion of compression along the threefold (111) axis[14], which induces the lowering of the  $O_h$  local symmetry to  $D_{3d}$ . In  $\text{VO}_2$  layers, the V-V geometry is built by two long ( $3.00781 \text{ \AA}$ ) and four short ( $2.99316 \text{ \AA}$ ) bonds in the IT phase, and reversely is by two short ( $2.97551 \text{ \AA}$ ) and four long ( $3.00526 \text{ \AA}$ ) ones in the LT phase[17]. The interlayer V-V distance is about  $5.6 \text{ \AA}$ .

All the calculations were performed by using the standard full-potential linearized augmented plane wave code WIEN2k[18]. The muffin-tin sphere radii of 2.22, 2.00 and 1.77 a.u. were chosen for the Na, V and O atoms, respectively. The cutoff parameter  $R_{mt}K_{max}$  was chosen to be 7.0 and 100  $k$ -points were used over the first Brillouin zone. The local spin density approximation (LSDA) of Perdew and Wang[19] was used for the exchange and correlation potential. In order to take the strong-correlated nature of  $3d$  electrons into account explicitly, we performed LSDA+ $U$  calculations[20], where  $U_{eff}=U-J$  ( $U$  and  $J$  are on-site Coulomb and exchange interaction respectively) was used instead of  $U$ [21]. And the orbital-dependent potential has the form of  $\Delta V_{FLL}$

$= -U_{eff}(\hat{n}^\sigma - \frac{1}{2}I)$ [22], where  $\hat{n}^\sigma$  is the orbital occupation matrix of spin  $\sigma$ . This type of double-counting correction (DCC) has been called the fully localized limit[23, 24]. For NaVO<sub>2</sub>, we used  $U_{eff}=3.6$  eV which has been used in its sister compound LiVO<sub>2</sub>[5]. Note also that the conclusion made in this paper is not affected for  $U_{eff}=2-6$  eV[25]. To explore the origin of small magnetic moment observed in the LT phase, we performed LSDA+SOC+U calculations, where the SOC is included by the second-variational method with scalar relativistic wave functions[18]. The easy magnetization direction was set along ( $\bar{1}10$ ) direction (short V-V bonds in the LT phase) observed in the experiment[14].

In order to investigate different magnetic patterns,  $2 \times 2 \times 2$  supercell was used in our calculations. We took into account two AFM structures in V-V plane as described in Fig. 2(a): I-type antiferromagnetism (Fig. 2(a)(i)) is AFM exchange along the (010) and ( $\bar{1}10$ ) directions with FM exchange along the (100) direction, II-type antiferromagnetism (Fig. 2(a)(ii)) is AFM exchange along the (100) and (010) directions with FM exchange along the ( $\bar{1}10$ ) direction. Totally there were five possible magnetic configurations in our calculations for the IT and LT phases (Fig. 2(b)): ferromagnetic (FM), C-AFI (I-type antiferromagnetism in plane, FM stacking), C-AFII (II-type antiferromagnetism in plane, FM stacking), G-AFI (I-type antiferromagnetism in plane, AFM stacking), G-AFII (II-type antiferromagnetism in plane, AFM stacking).

### III. RESULTS AND DISCUSSIONS

#### A. HT phase

As the paramagnetic behavior of NaVO<sub>2</sub> has been determined from the magnetic susceptibility measurements in the HT phase[14, 15], we just focus on the electronic structure instead of its magnetic properties.

The band structures obtained from LSDA and LSDA+U calculations are shown in Fig. 3. Within LSDA (Fig. 3(a)), the bands near the Fermi level ( $E_F$ ) are mainly derived from V  $3d$  states. Since straight V-O-V paths are not present in layered NaVO<sub>2</sub> and instead only nearly  $90^\circ$  V-O-V bonds exist, the V  $3d$  states are quite narrow. In the approximately octahedral crystal field, the  $3d$  orbitals are split into upper  $e_g$  and lower  $t_{2g}$  states. As shown in Fig. 3(a),  $e_g$  derived bands range from 1.5 to 2.5 eV and  $t_{2g}$  derived bands lie between -1.5 and 0.5 eV. The splitting between  $t_{2g}$  and  $e_g$  bands is about 1 eV. Under the trigonal crystal field, the  $t_{2g}$  orbitals are further split into

one  $a_{1g}$  and two degenerate  $e'_g$  orbitals. However, the splitting is much less than the band widths so that the  $t_{2g}$  orbitals still cross the  $E_F$ , which denotes a metallic state within LSDA. That is to say, LSDA calculations can not reproduce the insulating nature of  $\text{NaVO}_2$  from experiment[14]. The LSDA+U scheme[20] is thus used to count the strong correlation of V 3d electrons. As shown in Fig. 3(b), the empty  $a_{1g}$  band is pushed upwards by about 1 eV, and a gap is opened near the  $E_F$ . The system is hence an insulator due to electron correlation and  $\text{NaVO}_2$  is indeed a good candidate for Mott-Hubbard insulator.

According to the pure crystal field theory, the  $a_{1g}$  orbital is of lower energy than the  $e'_g$  orbitals under the trigonal distortion of compression, which is opposite to our LSDA+U results. So it is necessary to discuss the controversy on relative order of  $a_{1g}$ - $e'_g$  in such trigonal distortions. In Ref. [26], Landron and Lepetit pointed out that this relative order is strongly influenced by the  $e_g$ - $e'_g$  hybridization. The  $e_g$  and  $e'_g$  orbitals belong to the same irreducible representation ( $E_g$ ) and can thus mix despite the large  $t_{2g}$ - $e_g$  energy difference. Such a mix may be small but it modulates large energetic factors: the on-site Coulomb repulsions. When the  $e_g$ - $e'_g$  hybridization is taken into account, the energy difference  $\Delta E$  between the  $a_{1g}$  and  $e'_g$  orbitals depends on two competitive parts:  $\Delta E = \Delta E_1 + \Delta E_2 = \varepsilon(a_{1g}) - \varepsilon(e'_g)$ .  $\Delta E_1$  includes the kinetic energy, the electron-charge interaction, and the interaction with the core electrons.  $\Delta E_2$  denotes the repulsion and exchange terms within the 3d shells. Additionally,  $\Delta E_1$  and  $\Delta E_2$  both depend on the amplitude of the trigonal distortion and are of opposite effect with each other. Under a trigonal distortion of compression, if we only consider the crystal field effect ( $\Delta E_1$ ), the  $a_{1g}$  orbital is of lower energy than the  $e'_g$  orbitals ( $\Delta E < 0$ ). Whereas if we take  $\Delta E_2$  into account, the relative order between the  $a_{1g}$  and  $e'_g$  orbital is reversed ( $\Delta E > 0$ ), comparing with the crystal field prediction. Therefore, LSDA+U calculations predict that the  $a_{1g}$  orbital is of higher energy than the  $e'_g$  orbitals in  $\text{NaVO}_2$ . In fact, such a controversy has been presented in another compressed triangular system  $\text{Na}_x\text{CoO}_2$ [27, 28, 29]. From the crystal field theory, some authors[27] proposed that the energy of  $a_{1g}$  orbital is lower than the  $e'_g$  orbitals. However, the LDA+U method[28, 29] yielded an  $a_{1g}$  orbital of higher energy than the  $e'_g$  orbitals. Later, the experimental results[30] showed that the Fermi surface of the  $\text{CoO}_2$  layers issues from the  $a_{1g}$  orbital, not at all from the  $e'_g$  orbitals, supporting the LDA+U results.

## B. IT phase

The triangular lattice of NaVO<sub>2</sub> exhibits magnetic frustration and spatially anisotropic exchange interactions in the IT phase. As shown in Table II, the *G*-AFI configuration is the most stable state among the five magnetic structures both from LSDA and LSDA+U calculations. By a detailed analysis of the magnetic ground state *G*-AFI, see Fig. 2(a)(i), AFM chains are formed along the ( $\bar{1}10$ ) direction (long V-V bonds), while AFM exchange is also more favorable along the (010) direction (short V-V bonds). Considering all the short V-V bonds are completely equivalent, both of the (100) and (010) directions should be AFM exchange. Thus, NaVO<sub>2</sub> in the IT phase can be regarded as a system with frustration effects. In addition, spatially anisotropic exchange interactions may exist in such a triangular spin lattice[2], i.e.,  $J_1$  along the direction of long V-V bonds and  $J_2$  along the two directions of short V-V bonds (Fig. 2(a)(i)).

In order to describe the magnetic frustration and spatially anisotropic exchange interaction more clearly, we estimate the exchange interactions along one of the triangle directions ( $J_1$ ) and the other two ( $J_2$ ) (Fig. 2(a)(i)). Since all the configurations exhibit insulator characteristics, the spin size of V is stable, and the difference of total energy between *C*-AFI and *G*-AFI (*C*-AFII and *G*-AFII) configurations (See Table II) is so small that the system exhibits a 2D characteristic, a nearest neighbor Heisenberg-like Hamiltonian may be a good primary approximation for the in-layer magnetic energy. The corresponding 2D spin Hamiltonian can be written as

$$H = J_1 \sum_{(k,l)} \mathbf{S}_k \cdot \mathbf{S}_l + J_2 \sum_{(i,j)} \mathbf{S}_i \cdot \mathbf{S}_j \quad (1)$$

where  $(i,j)$  denotes a nearest-neighbor pair (short V-V bond) and  $(k,l)$  denotes a next-nearest-neighbor pair (long V-V bond). By mapping the obtained total energies for each magnetic state to the Heisenberg model, the exchange interactions  $J_1$  and  $J_2$  were calculated within this approximation:

$$2 \times (8 \times 4J_2S^2) = E(FM) - E(C - AFII) \quad (2)$$

$$2 \times (4 \times 4J_2S^2 + 4 \times 4J_1S^2) = E(FM) - E(C - AFI) \quad (3)$$

With  $S=1$ , we get  $J_2=2.1$  meV and  $J_1=6.1$  meV for NaVO<sub>2</sub> in the IT phase, which reflects strong spatial anisotropy. The AFM chains are established along the ( $\bar{1}10$ ) direction ( $J_1$ ) and the inter-chain coupling ( $J_2$ ) is frustrated. Moreover, the value of  $J_2/J_1=0.3$  is so small that this magnetic structure can be described as so-called weakly coupled *zigzag* ( $S=1$ ) chains model[31].

The integer spins ( $S=1$ ) are able to weaken the frustration effects in the frustrated systems, as in kagomé lattice[32]. Such a lattice has four nearest neighbors with the adjacent triangles on the lattice sharing only one lattice point. Interestingly, the triangular lattice can be composed of four kagomé lattices[27]. Thus, there are some analogous properties in these two frustrated systems. Therefore, it is reasonable to suppose that the triangular lattice also has the rule that the half-odd-integer spins are more highly frustrated than integer ones. For example,  $\text{NaTiO}_2$  ( $S = \frac{1}{2}$ )[5] and  $\text{LiCrO}_2$  ( $S = \frac{3}{2}$ )[6] with half-odd-integer spins are always frustrated even at low  $T$ , while the magnetic frustration of  $\text{NaMnO}_2$  ( $S=2$ ) is clearly lifted by a structural distortion[2]. Besides  $\text{NaMnO}_2$ ,  $\text{NaVO}_2$  is another typical triangular lattice with integer spins ( $S=1$ ). Therefore, we can presume that the magnetic frustration in  $\text{NaVO}_2$  can be lifted in some way.

### C. LT phase

From the discussion above, we expect that  $\text{NaVO}_2$  with  $S=1$  will show a long-range magnetic ordering or a finite ground-state magnetization at low  $T$ . As shown in Table II,  $G$ -AFII is only 0.3 meV lower in total energy than  $C$ -AFII within LSDA, and both  $G$ -AFII and  $C$ -AFII have the same lowest total energy from LSDA+U results for the LT phase. This reflects the obvious 2D characteristic of  $\text{NaVO}_2$ : the interlayer interaction is much weaker than the intralayer one. As stacking antiferromagnetically between layers is observed in the experiment[14],  $G$ -AFII state should be more favorable at low  $T$ . Such a magnetic state denotes the long range 3D magnetic ordering with AFM coupled FM chains in V cation layers and interlayer AFM coupling. Obviously, the magnetic frustration is lifted in  $G$ -AFII state by the first-order transition at 91.5 K: the lattice distorts to another monoclinic ( $C2/m$ ) with four long and two short V-V bonds reversed, comparing with IT phase.

The lattice distortion, which relieves the frustration, is driven by the formation of OO in the LT phase. Fig. 4 shows the orbital characteristic of V  $3d$  in  $G$ -AFII state. Since the orbital occupancies of the two inequivalent V (V1 and V2 in Fig. 2(a)(ii)) are nearly the same, only the density of states (DOS) of V1  $3d$  is shown. The  $z$  axis of local coordinate system coincides with the V-O bond of the  $\text{VO}_6$  octahedra. In such a coordinate system,  $d_{zx}$  and  $d_{yz}$  orbitals are mainly occupied and  $d_{xy}$  orbital is less occupied at all V ions. Such an orbital occupancy is consistent with the OO proposed by McQueen and Cava[14]: the  $d_{zx}$  and  $d_{yz}$  orbitals are singly occupied with all unoccupied  $d_{xy}$  orbitals.

This OO relieves the magnetic frustration and stabilizes the long-range magnetic ordering state. In view of the weak superexchange interaction resulted from the nearly  $90^\circ$  angle of V-O-V[33] as well as the weak magnetic interaction between adjacent  $\text{VO}_2$  planes interleaved by a layer of Na ions, the V-V direct exchange interaction in-plane should be dominant in such a particular crystal structure. Particularly, we only consider the  $\sigma$  overlap in V-V direct exchange, which is much stronger than the  $\pi$  overlap. It means that each orbital in a V ion only hybridizes with the same orbitals in the two nearest-neighboring V ions. That is to say,  $d_{yz}$  orbital hybridizes with two neighboring  $d_{yz}$  orbitals in the (010) and (0 $\bar{1}$ 0) directions, and  $d_{zx}$  orbital hybridizes with two neighboring  $d_{zx}$  orbitals in the (100) and ( $\bar{1}$ 00) directions. The repulsions between the occupied orbitals ( $d_{zx}$  or  $d_{yz}$ ) induce the elongation of V-V bonds along four directions: (010), (0 $\bar{1}$ 0), (100) and ( $\bar{1}$ 00). According to the Goodenough-Kanamori (GK) rules[34], the strong AFM coupling should exist along these four directions because of the occupation of two orbitals with  $\sigma$  overlap. At the same time, the less occupancy of  $d_{xy}$  orbital leads to V-V bonds contraction as well as a weak FM exchange along the (1 $\bar{1}$ 0) and ( $\bar{1}$ 10) directions. Thus, the four long and two short V-V bonds result from bonding via  $d_{zx}$ ,  $d_{yz}$  orbitals, but no bonding of the  $d_{xy}$  electrons. In other words, such an OO results in the lattice distortion, and consequently relieves the magnetic frustration.

In the LT phase, another important aspect is that the SOC turns out to be crucial for the small magnetic moment of  $0.98 \mu_B$  per  $\text{V}^{3+}$  observed experimentally[14]. As shown in Table II, the magnetic moments from LSDA+U calculations are much larger than the ones observed in the experiment. Further to investigate the magnetic moments changing with the particular choice of  $U_{eff}$ , we calculate the moments for  $U_{eff}=2-6$  eV and find that the moments are not sensitive to  $U_{eff}$ : as shown in Table III, the magnetic moments stay constant within  $0.2 \mu_B$  as long as the system is an insulator. Since an easy magnetization direction ( $\bar{1}$ 10) is observed in the experiment[14], the SOC may play an important role in determining the total magnetic moment. Thus, the SOC is included to reinvestigate the magnetic moment.

Then, we perform LSDA+SOC+U calculations for the favorable magnetic configuration ( $G$ -AFII), and obtain a local moment of  $0.89 \mu_B$  per  $\text{V}^{3+}$  with  $1.65 \mu_B$  spin and  $-0.77 \mu_B$  orbital contributions. This value is half the expected moment ( $2 \mu_B$ ), but very close to the observed one ( $0.98 \mu_B$ ). The DOS projected on (2,m) space shown in Fig. 5 reveals the origin of orbital moment. Note that the  $z$  axis is set to the direction of easy magnetization along ( $\bar{1}$ 10) now. Since  $d_1$  and  $d_{-1}$  have nearly the same occupancies, the orbital moment only comes from the contribution of different occupancies between  $d_2$  and  $d_{-2}$ . By further analysis, the  $d_2$  occupancy is less than



one half of the  $d_{-2}$  one, which should give an orbital moment between  $1 \mu_B$  and  $2 \mu_B$ . Nevertheless, there is no surprising that the calculated orbital moment is  $0.77 \mu_B$  here, because some hybridization effects are neglected in above analysis, e.g., the covalence effects with O  $2p$ . Thus, the inclusion of SOC leads to a surprising but experimentally sound results.

#### IV. CONCLUSIONS

In Summary, we have investigated the electronic structure and magnetic properties of  $\text{NaVO}_2$  by first-principles calculations. The  $t_{2g}$  orbitals are split into upper  $a_{1g}$  and lower  $e'_g$  states by a trigonal distortion of compression in the HT phase, which is similar to the splitting in  $\text{Na}_x\text{CoO}_2$ [28]. In the IT phase, the crystal symmetry is lowered to  $C2/m$ , under which the system behaves like a frustrated spin lattice with spatially anisotropic exchange interactions. Finally, a long-range ordered AFM ground state is formed when the magnetic frustration is relieved by another lattice distortion resulted from a certain ordering of occupied orbitals at low  $T$ . The small magnetic moment observed originates from the compensation of orbital moment for the spin moment. It is obvious that so many physical phenomena in the triangular lattice are reflected in  $\text{NaVO}_2$ , suggesting that  $\text{NaVO}_2$  is a very good model material for studying 2D triangular lattice systems.

#### V. ACKNOWLEDGEMENTS

We thank T. M. McQueen, P. W. Stephens, Q. Huang, T. Klimczuk, F. Ronning, and R. J. Cava for providing structural parameters prior to publication. This work was supported by the special Funds for Major State Basic Research Project of China(973) under grant No. 2007CB925004, 863 Project, Knowledge Innovation Program of Chinese Academy of Sciences, and Director Grants of CASHIPS, CUHK Direct Grant No. 2060345. Part of the calculations were performed in Center for Computational Science of CASHIPS and the Shanghai Supercomputer Center.

- 
- [1] K. Takada, H. Sakurai, E. Takayama-Muromachi, F. Izumi, R. A. Dilanian, and T. Sasali, Nature (London) **422**, 53 (2003).

- [2] Maud Giot, Laurent C. Chapon, John Androulakis, Mark A. Green, Paolo G. Radaelli, and Alexandros Lappas, *Phys. Rev. Lett.* **99**, 247211 (2007).
- [3] C. Darie, P. Bordet, S. de Brion, M. Holzapfel, O. Isnard, A. Lecchi, J. E. Lorenzo, and E. Suard, *Eur. Phys. J. B* **43**, 159 (2005).
- [4] F. Reynaud, D. Mertz, F. Celestini, J.-M. Debierre, A. M. Ghorayeb, P. Simon, A. Stepanov, J. Voiron, and C. Delmas, *Phys. Rev. Lett.* **86**, 3638 (2001).
- [5] S. Yu. Ezhov, V. I. Anisimov, H. F. Pen, D. I. Khomskii and G. A. Sawatzky, *Europhys. Lett.* **44**, 491 (1998).
- [6] I. I. Mazin, *Phys. Rev. B* **75**, 094407 (2007).
- [7] Albert J. W. Reitsma, Louis Felix Feiner and Andrzej M. Oleś, *New J. Phys.* **7**, 121 (2005).
- [8] F. Mila, F. Vernay, A. Ralko, F. Becca, P. Fazekas and K. Penc, *J. Phys.: Condens. Matter* **19**, 145201 (2007).
- [9] J.-H. Chung, Th. Proffen, S. Shamoto, A. M. Ghorayeb, L. Croguennec, W. Tian, B. C. Sales, R. Jin, D. Mandrus and T. Egami, *Phys. Rev. B* **71**, 064410 (2005).
- [10] Y. Tokura and N. Nagaosa, *science*, **288**, 462 (2000)
- [11] J.-Q. Yan, J.-S. Zhou, and J. B. Goodenough, *Phys. Rev. Lett.* **93**, 235901 (2004).
- [12] Peter Horsch, Andrzej M. Oleś, Louis Felix Feiner, and Giniyat Khaliullin, *Phys. Rev. Lett.* **100**, 167205(2008).
- [13] H. F. Pen, J. van den Brink, D. I. Khomskii, and G. A. Sawatzky , *Phys. Rev. Lett.* **78**, 1323 (1997).
- [14] T. M. McQueen, P. W. Stephens, Q. Huang, T. Klimczuk, F. Ronning, and R. J. Cava, *Phys. Rev. Lett.* **101**, 166402 (2008).
- [15] M. Onoda, *J. Phys. Condens. Matter* **20**, 145205 (2008).
- [16] H. F. Pen, L. H. Tjeng, E. Pellegrin, F. M. F. de Groot, G. A. Sawatzky, M. A. van Veenendaal and C. T. Chen, *Phys. Rev. B* **55**, 15500 (1997).
- [17] The difference between 93 K and 91.5 K has to do with the sample being measured on warming or on cooling. The IT to LT transition temperature is  $T=91.5$  K here, corresponding to the lattice parameters measured on cooling. And the slight lattice-parameter differences from Ref. [14] are within experimental error.
- [18] P. Blaha *et al.*, <http://www.wien2k.at>.
- [19] John P. Perdew and Yue Wang, *Phys. Rev. B* **45**, 13244 (1992).
- [20] Vladimir I. Anisimov, Jan Zaanen, and Ole K. Andersen, *Phys. Rev. B* **44**, 943 (1991).

- [21] S. L. Dudarev, G. A. Botton, S. Y. Savrasov, C. J. Humphreys and A. P. Sutton, Phys. Rev. B **57**, 1505 (1998).
- [22] G. K. H. Madsen and P. Novak, Europhys. Lett. **69**, 777 (2005).
- [23] V. I. Anisimov, I. V. Solovyev, M. A. Korotin, M. T. Czyżyk and G. A. Sawatzky, Phys. Rev. B **48**, 16929 (1993).
- [24] Robert Laskowski, Peter Blaha, and Karlheinz Schwarz, Phys. Rev. B **67**, 075102 (2003).
- [25] We performed LSDA+U calculations for the two most stable configurations (*G*-AFI and *G*-AFII) both in the IT and LT phases with  $U_{eff}=2, 3, 5, 6$  eV. The results show that the *G*-AFI (*G*-AFII) is always the most stable state in the IT (LT) phase in such  $U_{eff}$  range.
- [26] Sylvain Landron and Marie-Bernadette Lepetit, Phys. Rev. B **77**, 125106 (2008).
- [27] W. Koshibae and S. Maekawa, Phys. Rev. Lett. **91**, 257003 (2003).
- [28] Sylvain Landron and Marie-Bernadette Lepetit, Phys. Rev. B **74**, 184507 (2006).
- [29] Liang-Jian Zou, J.-L. Wang, and Z. Zeng, Phys. Rev. B **69**, 132505 (2004).
- [30] M. Z. Hasan, Y.-D. Chuang, D. Qian, Y. W. Li, Y. Kong, A. P. Kuprin, A.V. Fedorov, R. Kimmerling, E. Rotenberg, K. Rossnagel, Z. Hussain, H. Koh, N. S. Rogado, M. L. Foo, and R. J. Cava, Phys. Rev. Lett. **92**, 246402 (2004).
- [31] Zheng Weihong, Ross H. McKenzie and Rajiv R. P. Singh, Phys. Rev. B **59**, 14367 (1999).
- [32] Swapan K. Pati and C. N. R. Rao, J. Chem. Phys. **123**, 234703 (2005).
- [33] J. B. Goodenough, Phys. Rev. **117**, 1442 (1960).
- [34] J. B. Goodenough, *Magnetism and the Chemical Bond* (Interscience Publishers, New York, 1963); J. Kanamori, J. Phys. Chem. Solids **10**, 87 (1959).

TABLE I: The lattice parameters of NaVO<sub>2</sub> at 100, 91.5 and 20 K

Temperature	100 K	91.5 K	20 K
space group	<i>R-3m</i>	<i>C2/m</i>	<i>C2/m</i>
a(Å)	2.9959(1)	5.1758(1)	5.2223(2)
b(Å)	2.9959(1)	3.0078(1)	2.9755(1)
c(Å)	16.0996(1)	5.6340(1)	5.6492(3)
$\alpha$ (°)	90	90	90
$\beta$ (°)	90	107.629(1)	108.335(1)
$\gamma$ (°)	120	90	90
x,y,z(Na)	3a(0, 0, 0)	2a(0, 0, 0)	2a(0, 0, 0)
x,y,z(V)	3b(0, 0, 0.5)	2d(0, 0.5, 0.5)	2d(0, 0.5, 0.5)
x,y,z(O)	6c(0, 0, 0.2339(0))	4i(0.2368(7), 0, 0.6989(5))	4i(0.2296(5), 0, 0.7005(4))

TABLE II: The total energy  $E$  (meV/ (8f. u.)), magnetic moment  $M$  ( $\mu_B$ ) per  $V^{3+}$  and band gap  $E_g$  (eV) in different magnetic states.

		Configuration	FM	C-AFI	G-AFI	C-AFII	G-AFII
LSDA	IT (T=91.5 K)	$E$	514	4	0	128	132
		$M$	1.63	$\pm 1.37$	$\pm 1.37$	$\pm 1.34$	$\pm 1.34$
	LT (T=20 K)	$E$	574	152	156	4	0
		$M$	1.51	$\pm 1.35$	$\pm 1.35$	$\pm 1.38$	$\pm 1.38$
LSDA+U	IT (T=91.5 K)	$E$	329	65	0	192	189
		$M$	1.71	$\pm 1.65$	$\pm 1.65$	$\pm 1.66$	$\pm 1.66$
	$E_g$	1.1	1.2	1.1	1.4	1.5	
	$E$	395	286	288	0	0	
	LT (T=20 K)	$M$	1.71	$\pm 1.66$	$\pm 1.66$	$\pm 1.65$	$\pm 1.65$
		$E_g$	1.2	1.4	1.4	1.1	1.1

TABLE III: The band gap  $E_g$  (eV) and magnetic moment  $M$  ( $\mu_B$ ) per  $V^{3+}$  for different  $U_{eff}$  (eV) in  $G$ -AFII configuration.

$U_{eff}$	2	3	3.6	5	6
$E_g$	0.02	0.9	1.1	1.8	2.3
$M$	$\pm 1.57$	$\pm 1.63$	$\pm 1.65$	$\pm 1.69$	$\pm 1.71$

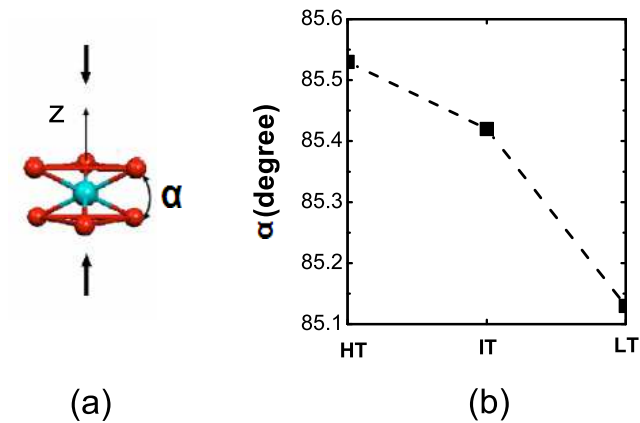
FIG. 1: (color online). (a) The compressed octahedron of  $\text{VO}_2$  layers. The  $z$  axis is the three fold axis of the  $\text{VO}_6$  octahedron.  $\alpha$  represents the O-V-O angle. (b)  $\alpha$  angles in the HT, IT and LT phases.

FIG. 2: (a) Two different magnetic patterns in V-V plane (i) I-type AF and (ii) II-type AF. The solid (dashed) lines represent short V-V bonds in the IT (LT) phase and dashed (solid) lines represent long V-V bonds in the IT (LT) phase.  $J_1$  ( $J_2$ ) denotes exchange interaction along the direction of dashed (solid) lines. (b) Schematic representation of five magnetic configurations used in our calculation. Only V atoms are drawn. Filled (open) circles indicate spin up (down) moments.

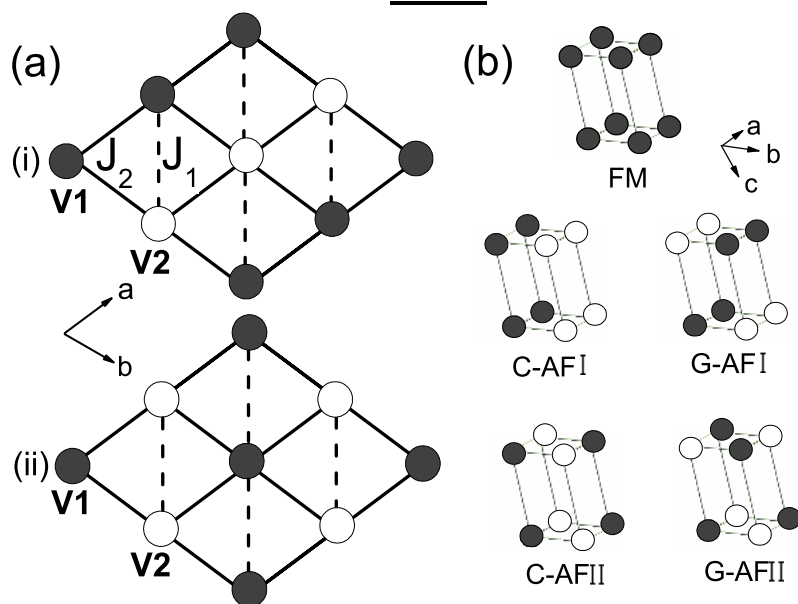
FIG. 3: The spin-majority band structure of  $\text{NaVO}_2$  from (a) LSDA and (b) LSDA+U ( $U_{eff}=3.6$  eV) calculations for the fixed structure at 100 K. The band with (a)  $3d$  and (b)  $a_{1g}$  character is marked.

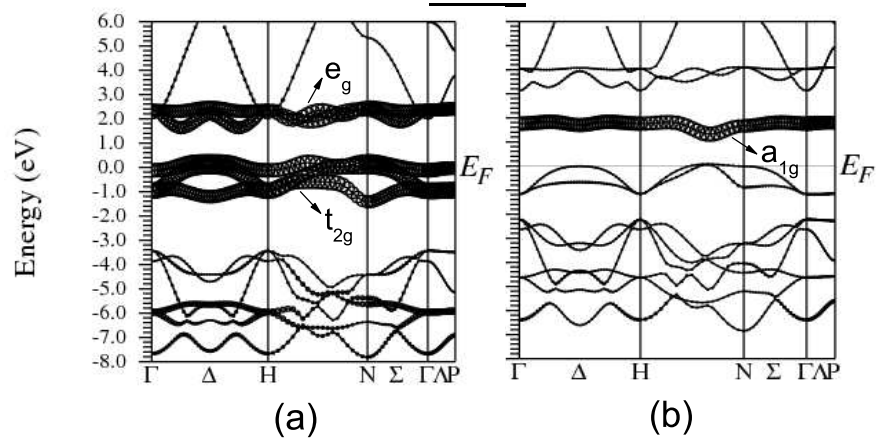
FIG. 4: Density of states (DOS) of  $\text{NaVO}_2$  calculated by LSDA+U ( $U_{eff}=3.6$  eV) in the  $G$ -AFII state for the fixed structure at 20 K. Besides total  $3d$  state, all the  $d_{zx}$ ,  $d_{yz}$  and  $d_{xy}$  orbitals in local coordinate system for V1 (Fig. 2(a)(i)) ion are depicted. Solid (dashed) lines denote the spin-up (down) states.

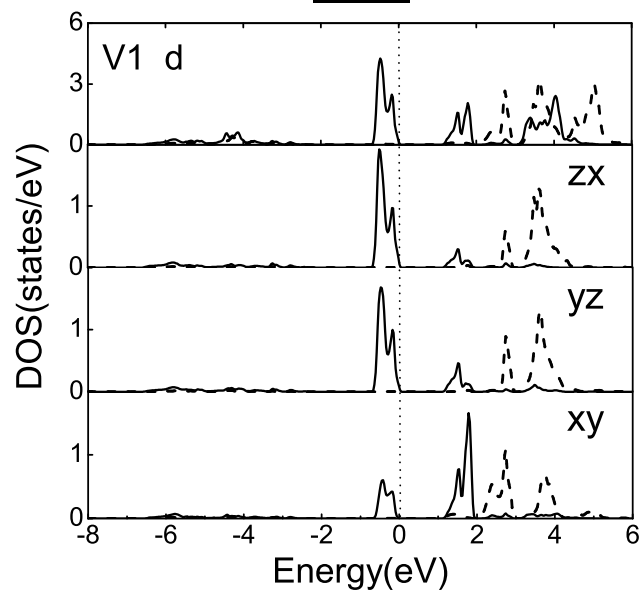
FIG. 5: Density of states (DOS) of  $\text{NaVO}_2$  calculated by LSDA+U+SOC ( $U_{eff}=3.6$  eV) in the  $G$ -AFII state for the fixed structure at 20 K. Solid (dashed) lines denote the spin-up (down) states.

**Fig. 1** tjia.eps



**Fig. 2** tjia.eps

**Fig. 3** tjia.eps

**Fig. 4** tjia.eps

**Fig. 5** tjia.eps